

RESEARCH

Open Access



# Prediction of pulmonary artery sling in children using echocardiography: scoring based on pulmonary artery bifurcation and pulmonary valve ring distance

Qiu-Chen Xu<sup>1†</sup>, Jian-Feng Liu<sup>2†</sup>, Min Xie<sup>1</sup>, Zong-Jie Weng<sup>1</sup>, Qiang Chen<sup>2\*†</sup> and Shan Guo<sup>1\*†</sup>

## Abstract

**Objective** To analyze the echocardiography characteristics of pulmonary artery sling (PAS) and explore the diagnostic value of the distance between the bifurcation of the left and right pulmonary arteries and the pulmonary artery valve annulus (DBP) in diagnosing PAS in children.

**Methods** This retrospective study analyzed echocardiographic data from 27 children diagnosed with PAS at our hospital from March 2014 to December 2022. The data were compared with those from 77 normal children. The study examined statistical differences between the two groups in the diameters of the left and right pulmonary arteries, the main pulmonary artery valve annulus diameter, and the DBP, both uncorrected and corrected for body surface area (BSA). The diagnostic utility of these measurements for distinguishing children with PAS from those without was assessed using receiver operating characteristic (ROC) curves.

**Results** The DBP and the corrected DBP values were significantly higher in the PAS group than in the normal group, with areas under the ROC curve of 0.909 for DBP and 0.951 for DBP/BSA ( $P < 0.05$ ). A DBP of 1.87 cm as the diagnostic threshold yielded a sensitivity of 98.9% and specificity of 84.4%. A DBP/BSA of 7.68 cm/m<sup>2</sup> had a sensitivity of 98.3% and specificity of 92.2%. The diagnostic odds ratios (OR) were 76.38% and 79.99%, respectively.

**Conclusion** The pivotal element in echocardiography diagnosis of PAS is the identification of the spatial relationship between the left pulmonary artery (LPA) and the trachea. The use of quantitative indices such as DBP and DBP/BSA for adjunctive diagnosis can positively impact the early detection of PAS.

<sup>†</sup>Qiu-Chen Xu and Jian-Feng Liu contributed equally to this work.

<sup>†</sup>Qiang Chen and Shan Guo are shared the corresponding authorship.

\*Correspondence:  
Qiang Chen  
chenqiang2228@163.com  
Shan Guo  
gs1f2005@163.com

Full list of author information is available at the end of the article



© The Author(s) 2025. **Open Access** This article is licensed under a Creative Commons Attribution-NonCommercial-NoDerivatives 4.0 International License, which permits any non-commercial use, sharing, distribution and reproduction in any medium or format, as long as you give appropriate credit to the original author(s) and the source, provide a link to the Creative Commons licence, and indicate if you modified the licensed material. You do not have permission under this licence to share adapted material derived from this article or parts of it. The images or other third party material in this article are included in the article's Creative Commons licence, unless indicated otherwise in a credit line to the material. If material is not included in the article's Creative Commons licence and your intended use is not permitted by statutory regulation or exceeds the permitted use, you will need to obtain permission directly from the copyright holder. To view a copy of this licence, visit <http://creativecommons.org/licenses/by-nc-nd/4.0/>.

### Graphical Abstract



Graphical Abstract. 1: the triangle symbol represents the pulmonary artery valve annulus; 2: The circular symbol indicates the bifurcation of the left and right pulmonary arteries; 3: The distance between the two markers represents the distance between the bifurcation of the left and right pulmonary arteries and the pulmonary artery valve annulus (DBP).

**Keywords** Pulmonary artery sling, Echocardiographic diagnosis, Pulmonary valve, Body surface area, Diagnostic odd ratio

### Introduction

Pulmonary artery sling (PAS) is considered a rare congenital anomaly, occurring in approximately 1 in 200,000 live births [1–2]. It is most commonly diagnosed in infancy or early childhood, though cases have also been reported in adults. PAS results from an abnormal embryonic development of the pulmonary arteries, leading to an anomalous course of the left pulmonary artery, which passes behind the trachea and/or esophagus instead of in front of them. While the specific cause of PAS is not always clear, it is believed to be associated with disruptions in the normal development of the embryonic vascular system during fetal growth. Additionally, genetic factors or underlying syndromes, such as 22q11.2 deletion syndrome (DiGeorge syndrome), may contribute to the development of PAS [3]. The severity of PAS

symptoms often varies based on the degree of tracheal or esophageal compression caused by the anomalous vessel. Treatment typically requires surgical correction to reposition the anomalous pulmonary artery and alleviate the compression on the trachea and/or esophagus [4–5].

Diagnosis of PAS in children typically relies on a mix of clinical evaluation and imaging studies. A chest X-ray may reveal signs such as an abnormal tracheal position, tracheal narrowing, and displacement of the esophagus. An echocardiography can provide detailed insights into the heart's structure, including the positioning of the pulmonary arteries and any related anomalies [6]. Computerized tomography angiography (CTA) is particularly effective in providing detailed images of the blood vessels, helping visualize the anatomy of the pulmonary arteries and their relationships with surrounding

structures. Magnetic resonance imaging (MRI) might also be utilized to further assess the anatomy when CT angiography is not feasible or to supply additional information [7].

Echocardiography is increasingly recognized as a fundamental diagnostic tool in intensive care unit, noted for its accessibility, non-invasive nature, repeatability, and versatility across various clinical indications [8]. However, the extent to which echocardiography contributes to increased sensitivity and specificity in diagnosing PAS remains to be fully determined. This study aims to evaluate the role of echocardiography in distinguishing between PAS and non-PAS abnormalities and to explore a quantitative index that could potentially aid in the diagnosis of PAS in children.

## Methods and materials

### Patients

This study is a single-center retrospective analysis that included 27 children who were diagnosed with PAS at our institution between March 2014 and December 2022, forming the PAS group. Additionally, 77 healthy children were included as the normal group. The study has been approved by the ethics committee.

### Echocardiography technique

Echocardiography examinations were conducted in a dimly lit echocardiography room to optimize image quality. The assessments utilized a digital premium cardiovascular ultrasound system (Philips IE33 and PHILIPS EPIQ 7 C, Highland Heights, OH, USA), equipped with real-time software and both S8-3 MHz and S5-18 MHz linear transducers. Children undergoing examination were positioned either supine or in the left lateral decubitus position. The scanning was performed through various acoustic windows including the parasternal, apical, subxiphoid, and suprasternal fossa. These windows facilitated the evaluation of several cardiovascular conditions and phenomena such as: (1) congenital malformations in the heart and great blood vessels; (2) irregular coordination of myocardial movement; (3) the status of blood flow through the valve and regurgitation, assessed using color Doppler imaging technology; (4) transvalvular pressure differences, determined by spectral Doppler technology.

### Data collection

The echocardiographic image storage system was accessed to retrieve and summarize measurement records, focusing on key anatomical dimensions: the inner diameter of the main pulmonary artery valve annulus (MPA), the inner diameters of the left (LPA) and right pulmonary arteries (RPA), and the distance from the bifurcation of both pulmonary arteries to the pulmonary valve annulus (DBP). All variations of the ultrasonic

sonographic characteristics from the PAS group, along with any associated cardiovascular malformations, were summarized and subjected to statistical comparison.

Demographic data such as gender, age, and weight of the enrolled children were collected. To mitigate the influence of age on the primary measured values, these were adjusted by division with the body surface area (BSA). The BSA is crucial for accurate dosing and measurement scaling [9–10]. This adjustment ensures that developmental variations across a diverse children's population do not skew the results. Additional imaging records, such as conventional CTA, were also reviewed as part of the comprehensive diagnostic approach.

### Statistical analysis

Statistical analyses were performed using SPSS software (version 16.0, New York, USA). Continuous variables that conformed to a normal distribution were described using means and standard deviations, and presented as (mean  $\pm$  SD). For those variables not normally distributed, median and interquartile ranges were used. Comparisons of continuous variables between groups were conducted using the rank sum test, while categorical data were expressed as numbers (n) and percentages (%), and analyzed using the chi-square ( $\chi^2$  [2]) test. Where appropriate, analysis of variance (ANOVA) or Pearson's chi-square test was applied to determine statistical significance. A two-sided *p*-value of  $<0.05$  was considered statistically significant.

To assess the diagnostic efficacy for PAS, receiver operating characteristic (ROC) curve analysis was utilized to determine the optimal cutoff value, based on the Youden index. The diagnostic accuracy of various measures for PAS was further evaluated by calculating sensitivity, specificity, positive likelihood ratio (LR+), negative likelihood ratio (LR-), and diagnostic odds ratio (DOR), along with their 95% confidence intervals (CIs). This comprehensive analytical approach was designed to rigorously evaluate the effectiveness of different diagnostic scores in identifying PAS.

## Results

The current study analyzed data from a total of 104 children. As shown in Table 1, the median age of patients in the PAS group was 67 days (IQR: 27.0, 222), while the median age in the normal group was 30 days (IQR: 12.5, 120). There were no differences between the two groups except DBP ( $2.94 \pm 0.75$  vs.  $1.63 \pm 0.51$ ,  $P < 0.05$ ) and DBP/BSA ( $10.58 \pm 2.40$  vs.  $5.75 \pm 1.31$ ,  $P < 0.05$ ).

Echocardiography for PAS revealed distinct abnormalities in the positioning of the LPA. Typically in the normal case, the pulmonary artery originates from the right ventricle and bifurcates into left and right branches. However, in PAS (Fig. 1A), the LPA arises from the RPA

**Table 1** The comparison of patients' information between PAS and control groups

	PAS group (n = 27)	Control group (n = 77)
Gender(boys/girls)	13/14	42/35
Age(days)	67(27.0, 222)	30(12.5, 120)
Weight(kg)	5.77±4.05	5.66±3.37
BSA (m <sup>2</sup> )	0.31±0.14	0.30±0.12
MPA(cm)	1.00±0.29	0.95±0.21
MPA/BSA(cm/ m <sup>2</sup> )	3.55±0.97	3.33±0.59
LPA(cm)	0.45±0.12	0.47±0.17
LPA/BSA(cm/ m <sup>2</sup> )	1.60±0.48	1.61±0.25
RPA(cm)	0.50±0.18	0.50±0.18
RPA/BSA(cm/m <sup>2</sup> )	1.74±0.58	1.70±0.27
DBP(cm)	2.94±0.75 *	1.63±0.51
DBP/BSA(cm/m <sup>2</sup> )	10.58±2.40 *	5.75±1.31

Note: BSA, body surface area. MPA, the inner diameter of the main pulmonary valve annulus. LPA, the inner diameter of the left pulmonary artery. RPA, the inner diameter of the right pulmonary artery. DBP, the distance from the bifurcation of both (left and right) pulmonary arteries to the pulmonary valve annulus. \*:  $P < 0.05$  vs. control group

and passes behind the highly echogenic trachea. Our study noted that in eight cases (29.6%), there was a right-deviated mediastinal PAS, attributed to hypoplasia of the right lung (Fig. 1B). This mediastinal shift to the right can cause the RPA to appear parallel to the longitudinal axis in the imaging, potentially leading to misinterpretation. It might be erroneously viewed as the typical MPA, with subsequent branches mistakenly identified as those of the LPA and RPA. For a more comprehensive understanding, Fig. 2 illustrates the echocardiographic characteristics and CTA images of standard PAS and cases with a right-deviated mediastinum. This comparison helps visualize the distinctions between the types of PAS, clarifying the unique presentations and aiding in accurate diagnosis and differentiation.

In the current study, 67% of the patients diagnosed with PAS also presented with various cardiac malformations.

These included ventricular septal defects (5 cases), atrial septal defects (5 cases), combined ventricular and atrial septal defects (2 cases), atrioventricular septal defects (1 case), pentalogy of Fallot and right aortic arch (1 case), and left superior vena cava (LSVC) (11 cases). Notably, 11 cases (40.7%) were associated with pulmonary hypertension, while 9 cases did not have accompanying cardiac malformations. Eight cases exhibited rightward deviation of the mediastinum PAS.

From the 104 cases reviewed, including 27 PAS cases, the data were used to calculate the area under the ROC (AUROC) for various measures: LPA/BSA (0.513), RPA/BSA (0.503), DBP (0.909), and DBP/BSA (0.951). The AUROC values for DBP and DBP/BSA were statistically significant ( $P < 0.01$  and  $< 0.001$  respectively), indicating a strong diagnostic performance (Table 2; Fig. 3). Two diagnostic cut-off values were determined: DBP at 1.87 cm and DBP/BSA at 7.68 cm/m<sup>2</sup>. The ROC for DBP/BSA, plotted to analyze diagnostic efficiency, revealed a diagnosis quality index of 89.8% for PAS (Fig. 4). Figure 5 shows the schematic diagram of PAS measurement in this study. In Fig. 5B, the DBP is significantly longer than in Fig. 5A, providing a more intuitive and quantifiable diagnostic clue for PAS.

Table 3 summarized the diagnostic performance of DBP and DBP/BSA score thresholds for detecting PAS. For DBP at the 1.87 cm cutoff value, the sensitivity and specificity were 98.9% and 84.4%, respectively. The positive and negative likelihood ratios were 7.17 (95% CI, 3.17–15.2) and 0.18 (95% CI, 0.06–0.32), respectively, with a diagnostic OR of 76.38 (95% CI, 39.21–89.16). For the DBP/BSA at the 7.68 cm/m<sup>2</sup> cutoff value, the sensitivity and specificity were 98.3% and 92.2%, respectively. The positive and negative LR were 8.09 (3.43–19.08) and 0.11 (0.03–0.21) respectively, with a diagnostic OR of 79.99 (95% CI, 46.21–98.98). This detailed statistical

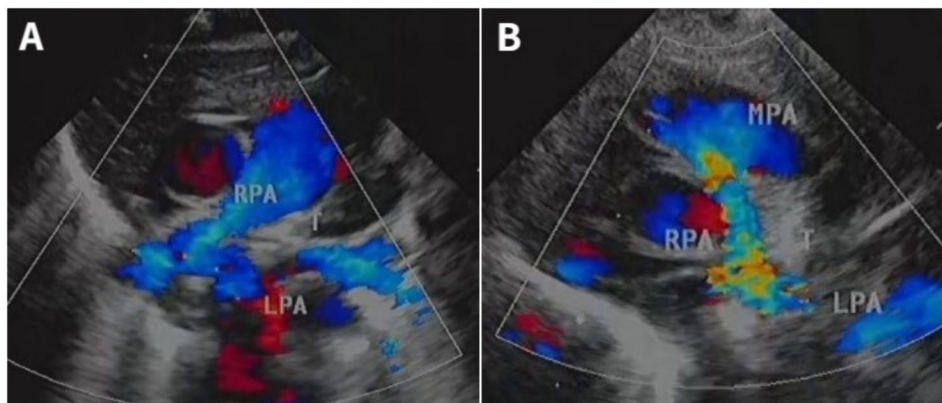


**Fig. 1** **A:** The typical PAS image (The RPA travels to the right, and the LPA originates from the RPA and travels to the left behind the trachea); **B:** Echocardiography of right-deviated mediastinum PAS (The RPA travels parallel to the longitudinal axis, the LPA originates from the RPA and travels to the left behind the trachea). (Note: LPA: left pulmonary artery, RPA: right pulmonary artery, MPA: main pulmonary artery, T: trachea)

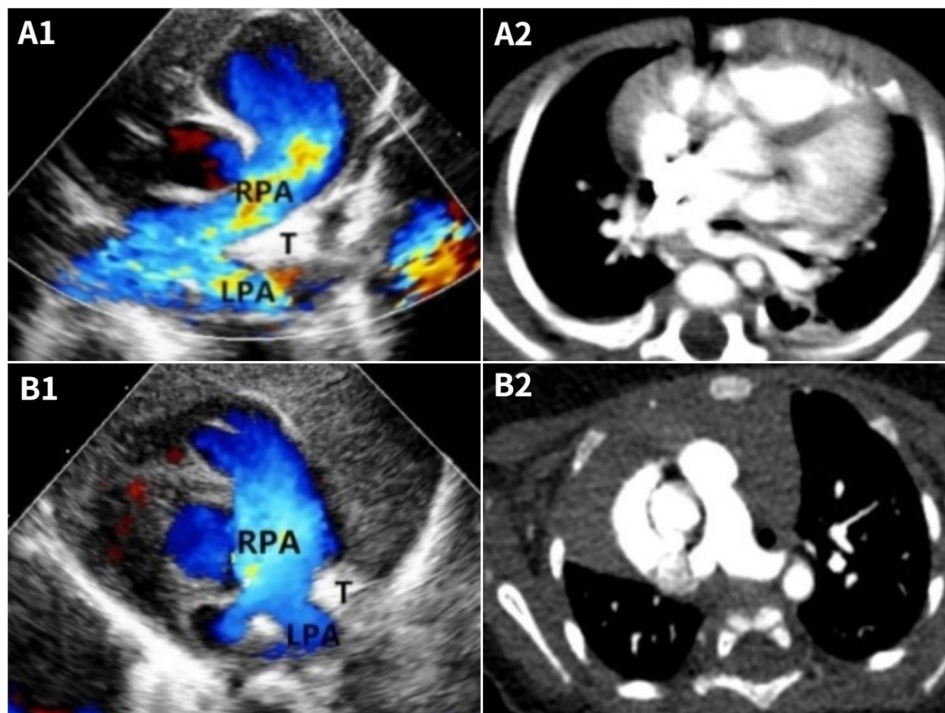


**Fig. 2** The echocardiographic characteristics and CTA images of PAS and right-deviated mediastinum PAS cases. A1: Color echocardiographic image; A2: CTA image; B1: Color echocardiographic image; B2: CTA image. (Note: LPA: left pulmonary artery, RPA: right pulmonary artery, T: trachea)

**Table 2** Characteristic plot (ROC) with different measurement values

Measurement Values	AUROC Score	Std. Error	The asymptotic significance	95% Confidence Interval
LPA/BSA	0.513	0.03	0.894	0.420, 0.639
RPA/BSA	0.503	0.03	0.976	0.404, 0.608
DBP	0.909	0.07	< 0.01	0.745, 1.03
DBP/BSA	0.951	0.07	< 0.001	0.806, 1.11

Note: AUROC, Area Under the Receiver Operating Characteristic Curve

evaluation highlights the robustness of DBP and DBP/BSA as effective metrics in the diagnosis of PAS.

The concordance between echocardiographic measurements and CT measurements is summarized in Table 4. The intraclass correlation coefficients (ICCs) demonstrate excellent agreement across all comparison groups. Specifically, the ICC for echocardiographic DBP measurements compared to CT measurements is 0.945 ( $P < 0.001$ ). Similarly, the ICC for echocardiographic LPA measurements compared to CT measurements is 0.929 ( $P < 0.001$ ), while the ICC for echocardiographic RPA measurements compared to CT measurements is 0.937 ( $P < 0.001$ ).

### Discussion

PAS is a congenital malformation where a branch pulmonary artery originates from the contralateral pulmonary artery. Since its initial report by Glaevecke and Doehle in 1897, PAS has been extensively studied [11–13]. Although CT scanning has become the preferred diagnostic method due to its ability to image airways and vessels clearly, its use is limited by its lack of accessibility, non-portability, and the risks associated with ionizing radiation, making it less suitable for early diagnosis of PAS [14]. In contrast, echocardiography, which is highly accessible, portable, uses non-ionizing radiation, and does not require sedation, is the ideal modality for early diagnosis of PAS [15–16]. Echocardiography also enables the concurrent diagnosis of associated congenital heart defects. However, clear diagnostic criteria for echocardiographic identification of PAS are currently lacking. To address this gap, we conducted a retrospective analysis of the echocardiographic characteristics of PAS in children. Our study found that 29.6% of the patients in our cohort exhibited a mediastinal shift to the right due to underdevelopment of the right lung, and 67% presented with various congenital heart defects. The results suggest that DBP and DBP/BSA have strong diagnostic efficacy for echocardiographically diagnosing PAS, with diagnostic thresholds of 1.87 cm and 7.68 cm/m<sup>2</sup>, respectively.

When diagnosing PAS via echocardiography, viewing the pulmonary artery bifurcation is critical. This view

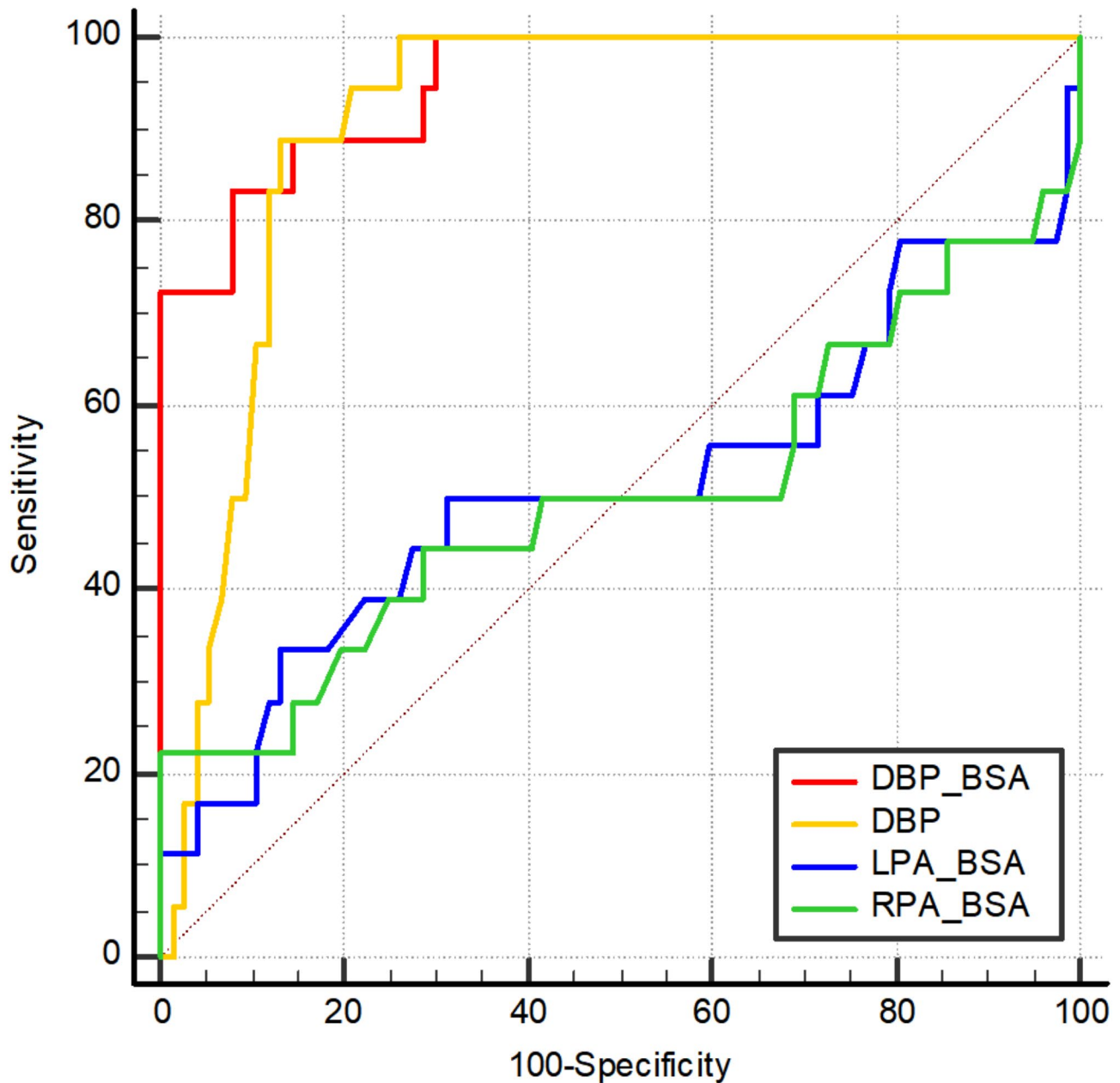


**Fig. 3** Characteristic plot (ROC) with different measurement values

typically reveals the anomalous origin of the LPA from the RPA, passing behind the trachea—a direct indicator for confirming PAS. Accurately determining the spatial relationship between the trachea and the LPA is a key diagnostic step. Echocardiographic studies on PAS have predominantly been conducted during the fetal period, where the trachea, filled with amniotic fluid, appears as an anechoic area on the images, facilitating the recognition of structures. In contrast, the neonatal trachea, filled with air, shows high echogenicity, often merging with surrounding lung tissue or connective tissue, which increases the difficulty of identification [17–18]. In our

study, 29.6% of PAS patients exhibited a mediastinal shift to the right due to underdevelopment of the right lung, aiding in the accurate diagnosis and differentiation of this condition. In this type of PAS, the RPA does not extend to the right as typical but may continue directly backward from the MPA. This causes the subsequent LPA and the distal RPA to appear similar to the normal bifurcation of the left and right pulmonary arteries. Misidentification of the strongly echogenic trachea anterior to the LPA can lead to diagnostic errors. such situations are commonly encountered in our clinical practice. The origins of the left and right pulmonary arteries are not always in the

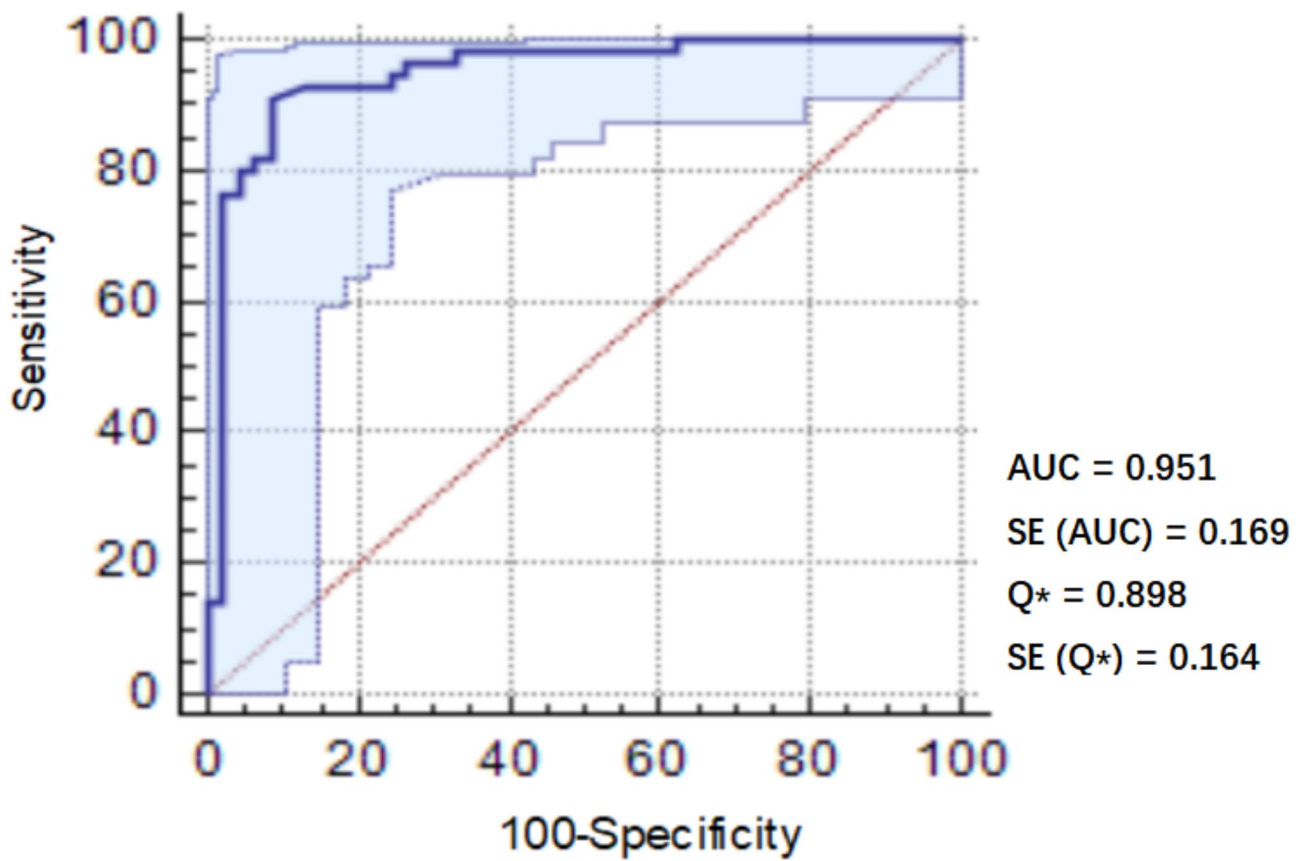


**Fig. 4** Summary DBP/BSA characteristic plot (ROC) for assessing diagnostic accuracy with corresponding curves indicative of upper and lower bounds of 95% CI. (AUC=area under curve, SE=standard error, Q\*=summary measure of accuracy derived from the ROC curve)

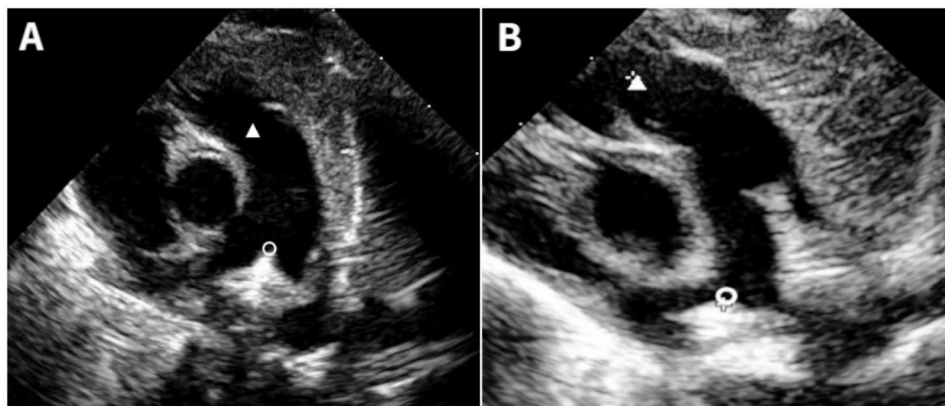


**Fig. 5** Echocardiography measurement diagram of PAS. Although the two images above look very similar, the DBP in Fig. 5B is significantly longer than in Fig. 5A, providing an intuitive and quantifiable diagnostic clue for PAS

**Table 3** Summary of estimates of diagnostic performance of DBP and DBP/BSA score threshold (1.87 cm and 7.68 cm/m<sup>2</sup>) for detecting PAS

	Sensitivity, % (95% CI)	Specificity, % (95% CI)	Positive LR (95% CI)	Negative LR (95% CI)	Diagnostic OR (95% CI)
BPD(cm)	98.9 (98.24–99.7)	84.4 (79.3–88.2)	7.17 (3.17–15.2)	0.18 (0.06–0.32)	76.38 (39.21–89.16)
BPD/BSA (cm/m <sup>2</sup> )	98.3 (96.2–99.5)	92.2 (88.1–98.7)	8.09 (3.43–19.08)	0.11 (0.03–0.21)	79.99 (46.21–98.98)

Note: LR, the likelihood ratio. OR, odds ratio

**Table 4** Concordance between echocardiographic measurements and CT measurements

Comparison group	ICC	P value
Exam 1* versus CT measurements	0.945	<0.001
Exam 2* versus CT measurements	0.929	<0.001
Exam 3* versus CT measurements	0.937	<0.001

\*Exam 1: DBP: the distance from the bifurcation of both pulmonary arteries to the pulmonary valve annulus; Exam 2: LPA: the inner diameters of the left pulmonary arteries; Exam 3: RPA: the inner diameters of the right pulmonary arteries

same horizontal plane; the left pulmonary artery usually arises slightly higher than the right pulmonary artery, but they do not cross each other. In these cases, the origins of the two pulmonary arteries remain relatively close, and by rotating the ultrasound probe, it is still possible to identify the bifurcation of the pulmonary arteries and measure the DBP. When the origin of the left pulmonary artery is slightly higher and rotates to the right wall of the main pulmonary artery, the initial segments of the left and right pulmonary arteries exhibit a crossed relationship, which is referred to as crossed pulmonary arteries. Even in cases with a clear diagnosis of crossed pulmonary arteries, the bifurcation of the left and right pulmonary arteries can still be located, allowing for accurate DBP measurement. Encountering cases of mediastinal shift type PAS and lacking experience in identifying the trachea, the bifurcation elongation sign can provide a very intuitive and quantifiable diagnostic clue (Fig. 5). When PAS patients also have concurrent congenital heart defects, it complicates the clinical course, affecting the complexity of surgical repair and prognosis. Previous studies have shown that the incidence of congenital heart defects in PAS patients ranges from 40 to 80%, with the most common defects being ventricular septal defects, atrial septal defects, and patent ductus arteriosus [19]. In our study, 67% of PAS patients also suffered from congenital heart defects, with incidence rates and types similar to those reported in previous research. A portion of patients with PAS may have a PDA that has not yet closed. Therefore, accurately identifying the PDA and LPA is crucial for locating the pulmonary artery bifurcation and measuring the DBP. Based on our clinical experience with such cases, we have found that anatomically, the origin of the PDA is slightly higher than that of the LPA. Additionally, the PDA is shorter, and echocardiographic can trace its connection to the descending aorta, which allows for confirmation that the vessel is a PDA and not an LPA—this is a key distinguishing feature. Furthermore, in most patients without pulmonary hypertension, the blood flow in the PDA is left-to-right (from the descending aorta through the PDA into the pulmonary artery), whereas the blood flow in the LPA is directed from the main pulmonary artery to the left pulmonary artery. Thus, the blood flow directions of the PDA and

LPA are opposite, and this can be observed on color Doppler ultrasound. However, it is important to note that in cases with pulmonary hypertension, the reversed blood flow direction can no longer serve as a reliable distinguishing feature.

In children with PAS, the LPA abnormally originates from the RPA instead of distally from the MPA. Theoretically, the distance between the bifurcation of the LPA and RPA from the MPA annulus should be longer in PAS patients than in normal children. The results of our study support this hypothesis and introduce an innovative method for echocardiographic diagnosis of PAS using DBP and DBP/BSA. Considering that some PAS cases are also diagnosed during childhood, our study population was specifically the children group [20]. Therefore, DBP/BSA offers higher diagnostic accuracy, making it a reliable method for diagnosing PAS in this demographic. Both measures exhibited high sensitivity and specificity, with the DBP/BSA measurement proving slightly superior. This likely reflects that while PAS most commonly occurs in newborns or infants, cases in older children have been reported. As age and weight increase, DBP also rises; thus, the area under the AUROC of DBP/BSA is higher, offering greater clinical applicability.

To our knowledge, this is the first time such a non-invasive method has been used to significantly enhance the diagnostic sensitivity and specificity for pediatric PAS. The quantitative indices DBP and DBP/BSA effectively address the challenges of misdiagnoses or missed diagnoses of PAS cases, which can occur due to insufficient experience in recognizing tracheal echoes. This approach potentially reduces unnecessary medical costs and the risk of complications associated with more invasive diagnostic procedures. Echocardiographic evaluation goes beyond merely assessing the size and branching patterns of the pulmonary arteries; it also effectively visualizes the abnormal positioning or origins of these arteries characteristic of PAS [21–22]. Our retrospective study provides real-time images of the heart and surrounding structures, enabling pediatric radiologists and clinical professionals to accurately detect the position of the pulmonary arteries and effectively manage cases.

## Conclusion

The pivotal element in echocardiography diagnosis of PAS is the identification of the spatial relationship between the LPA and the trachea. The use of quantitative indices such as DBP and DBP/BSA for adjunctive diagnosis can positively impact the early detection of PAS.

## Abbreviations

PAS	Pulmonary artery sling
LPA	Left pulmonary artery
RPA	Right pulmonary artery
CTA	Computerized tomography angiography

BSA	Body surface area
DBP	Distance between left and right pulmonary artery bifurcation and pulmonary valve
LR	Likelihood rate

### Acknowledgements

We highly acknowledge all the staff of our department.

### Author contributions

Qiu-Chen Xu and Shan Guo designed the study, performed the statistical analysis, participated in the operation, and drafted the manuscript. Jian-Feng Liu, Min Xie, and Zong-Jie Weng collected the clinical data. Qiang Chen and Shan Guo supervised the study. All authors read and approved the final manuscript.

### Funding

There is no funding.

### Data availability

No datasets were generated or analysed during the current study.

### Declarations

#### Ethics approval and consent to participate

This study was approved by the ethics committee of Fujian Maternity and Child Health Hospital and followed the guidelines outlined in the Declaration of Helsinki. Informed consent was waived by the Ethics Committee due to the retrospective nature of the study, as it posed minimal risk to participants and all data were analyzed anonymously, ensuring confidentiality.

#### Competing interests

The authors declare no competing interests.

#### Author details

<sup>1</sup>Department of Medical Ultrasonics, College of Clinical Medicine for Obstetrics & Gynecology and Pediatrics, Fujian Maternity and Child Health Hospital, Fujian Medical University, Fuzhou, China

<sup>2</sup>Department of Cardiac Surgery, College of Clinical Medicine for Obstetrics & Gynecology and Pediatrics, Fujian Children's Hospital (Fujian Branch of Shanghai Children's Medical Center), Fujian Medical University, Fuzhou, China

Received: 8 August 2024 / Accepted: 27 January 2025

Published online: 01 April 2025

### References

- Freedom RM, Yoo SJ, Mikailian H, Williams WG. The natural and modified history of congenital heart disease. New York, NY: Wiley-Liss; 2003. pp. 2633–82.
- Wells TR, Gwinn JL, Landing BH, Stanley P, Mandell GA. Congenital tracheal stenosis with bronchial malacia and airway compression by an anomalous innominate artery. *J Pediatr*. 1985;107(5):715–22.
- Momma K, Matsuoka R, Takao A. Aortic arch anomalies associated with chromosome 22q11 deletion (CATCH 22). *Pediatr Cardiol*. 1999;20:97–102.
- Senocak F, Ozme S, Bilici A, et al. Pulmonary artery sling: results of surgical treatment. *Surg Today*. 2009;39(2):118–23.
- Fiore AC, Brown JW, Weber TR, Turrentine MW. Surgical treatment of pulmonary artery sling and tracheal stenosis. *Ann Thorac Surg*. 2005;79:38–46.
- Ko H, Kim YH, Yoo SJ. Echocardiographic assessment of congenital heart disease: an echocardiographer's perspective. *Korean J Radiol*. 2016;17(5):560–80.
- van Son JA, Julsrud PR, Hagler DJ, et al. Repair of symptomatic pulmonary artery sling in infancy. *J Thorac Cardiovasc Surg*. 1994;107:1083–90.
- Močnik M, Marčun Varda N. echocardiography Elastography in Children. *Child (Basel)*. 2023;10(8):1296.
- Meban C. The surface area and volume of the human fetus. *J Anat*. 1983;137(Pt 2):271–8.
- Carolina Witchmichen Pentead Schmidt. *Body Surface Area (BSA)*, Pediatric Oncologic Pharmacy. 2019 ISBN: 978-3-030-10987-5.
- Binsalimah ZM, Thomason A, Ibarra C, Spigel Z, Adachi I, Barton KE, Edmunds E, Caldarone CA, Imamura M, Heinle JS. Midterm outcomes of pulmonary artery sling repair with and without tracheoplasty. *Cardiol Young*. 2021;31(1):52–9.
- Shen X, Tan W, Jia B, Ye M. Relationship between a Tracheal and Left Pulmonary Artery Stenosis Index and the prognosis of Pulmonary Artery Sling with Tracheal Stenosis. *Pediatr Cardiol*. 2021;42(7):1585–93.
- Yu JM, Liao CP, Ge S, Weng ZC, Hsiung MC, Chang JK, Chen FL. The prevalence and clinical impact of pulmonary artery sling on school-aged children: a large-scale screening study. *Pediatr Pulmonol*. 2008;43(7):656–61.
- Leonardi B, Secinaro A, Cutrera R, Albanese S, Trozzi M, Franceschini A, Silvestri V, Tomà P, Carotti A, Pongiglione G. Imaging modalities in children with vascular ring and pulmonary artery sling. *Pediatr Pulmonol*. 2015;50(8):781–8.
- Močnik M, Golob Jančič S, Marčun Varda N. Liver and kidney echocardiography in children and young adults with hypertension or chronic kidney disease. *Pediatr Nephrol*. 2023;38(10):3379–87.
- Olivier Villemain Jérôme, Baranger MK, Friedberg A, Dizeux E, Messas M, Tanter. Mathieu Pernot, Luc Mertens. *Ultrafast echocardiography Imaging in Pediatric and Adult Cardiology: Techniques, Applications, and Perspectives*. *JACC: Cardiovascular Imaging* 2020;13(8):1771–1791.
- Pawluś A, Sokołowska-Dąbek D, Szymańska K, Inglot MS, Zaleska-Dorobisz U. Echocardiography elastography—review of techniques and its clinical applications in Pediatrics—Part 1. *Adv Clin Exp Med*. 2015;24(3):537–43.
- Zaleska-Dorobisz U, Pawluś A, Szymańska K, Łasecki M, Ziajkiewicz M. Echocardiography elastography—review of techniques and its clinical applications in Pediatrics—Part 2. *Adv Clin Exp Med*. 2015;24(4):725–30.
- Xie J, Juan YH, Wang Q, Chen J, Zhuang J, Xie Z, Liang C, Zhu Y, Yu Z, Li J, Saboo SS, Liu H. Evaluation of left pulmonary artery sling, associated cardiovascular anomalies, and surgical outcomes using cardiovascular computed tomography angiography. *Sci Rep*. 2017;7:40042.
- Rahmath K, Durward MR. Pulmonary artery sling: an overview. *Pediatr Pulmonol*. 2023;58(5):1299–309.
- Lai WW, Geva T, Shirali GS, et al. Guidelines and standards for performance of a pediatric echocardiogram: a report from the Task Force of the Pediatric Council of the American Society of Echocardiography. *J Am Soc Echocardiogr*. 2006;19(12):1413–30.
- Lai WW, Mertens LL, Cohen MS, Geva T, editors. *Echocardiography in pediatric and congenital heart disease: from fetus to adult*. Wiley; 2016.

### Publisher's note

Springer Nature remains neutral with regard to jurisdictional claims in published maps and institutional affiliations.